AMERICAN SOCIETY FOR MICROBIOLOGY | Applied and Environmental Microbiology®

BIOTECHNOLOGY

Metabolic Engineering of *Raoultella ornithinolytica* BF60 for Production of 2,5-Furandicarboxylic Acid from 5-Hydroxymethylfurfural

Gazi Sakir Hossain,[a,b] Haibo Yuan,[b,c] Jianghua Li,[c] Hyun-dong Shin,[d] Miao Wang,[a] Guocheng Du,[b,c] Jian Chen,[c] Long Liu[b,c]

School of Food Science and Technology, Jiangnan University, Wuxi, China[a]; Key Laboratory of Carbohydrate Chemistry and Biotechnology, Ministry of Education, Jiangnan University, Wuxi, China[b]; Key Laboratory of Industrial Biotechnology, Ministry of Education, Jiangnan University, Wuxi, China[c]; School of Chemical and Biomolecular Engineering, Georgia Institute of Technology, Atlanta, Georgia, USA[d]

ABSTRACT 2,5-Furandicarboxylic acid (FDCA) is an important renewable biotechnological building block because it serves as an environmentally friendly substitute for terephthalic acid in the production of polyesters. Currently, FDCA is produced mainly via chemical oxidation, which can cause severe environmental pollution. In this study, we developed an environmentally friendly process for the production of FDCA from 5-hydroxymethyl furfural (5-HMF) using a newly isolated strain, *Raoultella ornithinolytica* BF60. First, *R. ornithinolytica* BF60 was identified by screening and was isolated. Its maximal FDCA titer was 7.9 g/liter, and the maximal molar conversion ratio of 5-HMF to FDCA was 51.0% (mol/mol) under optimal conditions (100 mM 5-HMF, 45 g/liter whole-cell biocatalyst, 30°C, and 50 mM phosphate buffer [pH 8.0]). Next, *dcaD*, encoding dicarboxylic acid decarboxylase, was mutated to block FDCA degradation to furoic acid, thus increasing FDCA production to 9.2 g/liter. Subsequently, *aldR*, encoding aldehyde reductase, was mutated to prevent the catabolism of 5-HMF to HMF alcohol, further increasing the FDCA titer, to 11.3 g/liter. Finally, the gene encoding aldehyde dehydrogenase 1 was overexpressed. The FDCA titer increased to 13.9 g/liter, 1.7 times that of the wild-type strain, and the molar conversion ratio increased to 89.0%.

IMPORTANCE In this work, we developed an ecofriendly bioprocess for green production of FDCA in engineered *R. ornithinolytica*. This report provides a starting point for further metabolic engineering aimed at a process for industrial production of FDCA using *R. ornithinolytica*.

KEYWORDS 2,5-furandicarboxylic acid, 5-hydroxymethyl furfural, *Raoultella ornithinolytica* BF60, metabolic engineering, whole-cell biocatalyst

A natural dicarboxylic acid derived from biomass, 2,5-furandicarboxylic acid (FDCA), is a promising new biotechnological building block with an enormous market potential. The U.S. Department of Energy has listed FDCA as one of the top 12 value-added chemicals obtained from biomass. A healthy human body produces 3 to 5 mg of FDCA per day. FDCA was first prepared by reacting mucic acid with fuming hydrobromic acid under pressure (1). The most important application of FDCA is its use as a building block in polyester production (2). FDCA is a promising replacement of terephthalic acid, which is used extensively for production of various polyesters, such as polyethylene terephthalate and polybutylene terephthalate (3). In addition, the diethyl ester of FDCA has been used pharmacologically as a strong anesthetic, whereas the dicalcium salt of FDCA and FDCA-derived anilides have been shown to inhibit

Received 5 August 2016 **Accepted** 17 September 2016

Accepted manuscript posted online 21 October 2016

Citation Hossain GS, Yuan H, Li J, Shin H, Wang M, Du G, Chen J, Liu L. 2017. Metabolic engineering of *Raoultella ornithinolytica* BF60 for production of 2,5-furandicarboxylic acid from 5-hydroxymethylfurfural. Appl Environ Microbiol 83:e02312-16. https://doi.org/10.1128/AEM.02312-16.

Editor Maia Kivisaar, University of Tartu

Address correspondence to Long Liu, longliu@jiangnan.edu.cn.

the growth of *Bacillus megaterium* (4). FDCA is used in medicine for removal of kidney stones because it can chelate various ions, including Ca^{2+}, Cu^{2+}, and Pb^{2+} (5). FDCA, being a very stable compound, is also an ingredient of fire foams. Through a reaction with diamines, FDCA can yield a new family of nylons derived completely from biomass (6).

Renewable carbon sources such as lignocellulosic biomasses may be good sources of 5-hydroxymethyl furfural (5-HMF) (7, 8). They could replace fossil sources, thus decreasing the demand for crude oil reserves and the associated greenhouse gas emissions. 5-HMF contains two functional groups and a furan aromatic ring. As a result, 5-HMF is a promising starting material for numerous chemical applications, including FDCA production.

Several chemical processes have been proposed for oxidative production of FDCA from 5-HMF (see Fig. S1 in the supplemental material). Most of these processes are performed at elevated temperatures and pressure and require the use of identical metal salts, such as cobalt or manganese, or different metal catalysts, such as Pd/Au or organic polymers loaded with iron (9, 10). In addition, the known chemical processes produce a mixture of FDCA, intermediate oxidation products, and side products. Consequently, the chemical production process requires an extra purification step, which increases the expense and reduces the output. In comparison with the chemical-synthesis-based production processes, biochemical production of FDCA from 5-HMF is less well established.

Recently, a furfural/HMF oxidoreductase was isolated from the bacterium *Cupriavidus basilensis* HMF14. This enzyme uses molecular oxygen to convert 5-HMF to FDCA, producing hydrogen peroxide as a by-product (11). Usually, hydrogen peroxide is toxic to the bacterial cell and to cellular metabolism. When engineered to express the furfural/HMF oxidoreductase, *Pseudomonas putida* can convert 5-HMF to FDCA, with a titer of 30 g/liter (12). On the other hand, *P. putida* also converts FDCA to α-ketoglutarate via the Trudgill pathway for use in the tricarboxylic acid (TCA) cycle (11). Thus, there is a need for a natural biocatalyst that can convert 5-HMF to FDCA without producing toxic compounds and that can tolerate a high concentration of 5-HMF, which is toxic to living cells. In addition, during the production of FDCA, its degradation and the conversion of HMF to other unusable metabolic products, such as an alcohol, must be blocked. In recently published studies, specifically based on analysis of *Cupriavidus basilensis*, it was reported that 5-HMF is converted to 5-furfural-2-carboxylic acid (FFCA) and HMF alcohol primarily (11–13). Then, FFCA is converted to FDCA, which is degraded via 2-furoic acid to 2-ketoglutarate by different enzymes and ultimately is consumed by the microbes via the TCA cycle. On the basis of these available data, Fig. 1 shows the metabolic pathway for FDCA production from 5-HMF, with product and substrate utilization.

Raoultella is a genus that comprises Gram-negative, facultative anaerobic organisms that are oxidase negative and have both fermentative and respiratory types of metabolism. This genus was named after the French bacteriologist Didier Raoult and belongs to the *Enterobacteriaceae* family. Phylogenetic analysis of the 16S rRNA and *rpoB* genes shows that *Raoultella* derives from the genus *Klebsiella* (14, 15). However, no study has specifically shown the production of FDCA by using *Raoultella* sp.

In the present study, a new bacterial strain, *R. ornithinolytica* BF60, was isolated on the basis of its ability to produce FDCA from 5-HMF. The production process was then optimized. Thereafter, *dcaD*, encoding dicarboxylic acid decarboxylase, and *aldR*, encoding aldehyde reductase, were mutated to block FDCA degradation and the conversion of 5-HMF to HMF alcohol, respectively. Finally, the gene encoding aldehyde dehydrogenase 1 was overexpressed to improve the production of FDCA by the engineered *R. ornithinolytica* BF60 strain.

RESULTS

Characterization of the new strain *R. ornithinolytica* BF60. To identify the strain, which is 5-HMF tolerant and produces FDCA from 5-HMF, a soil sample collected at a

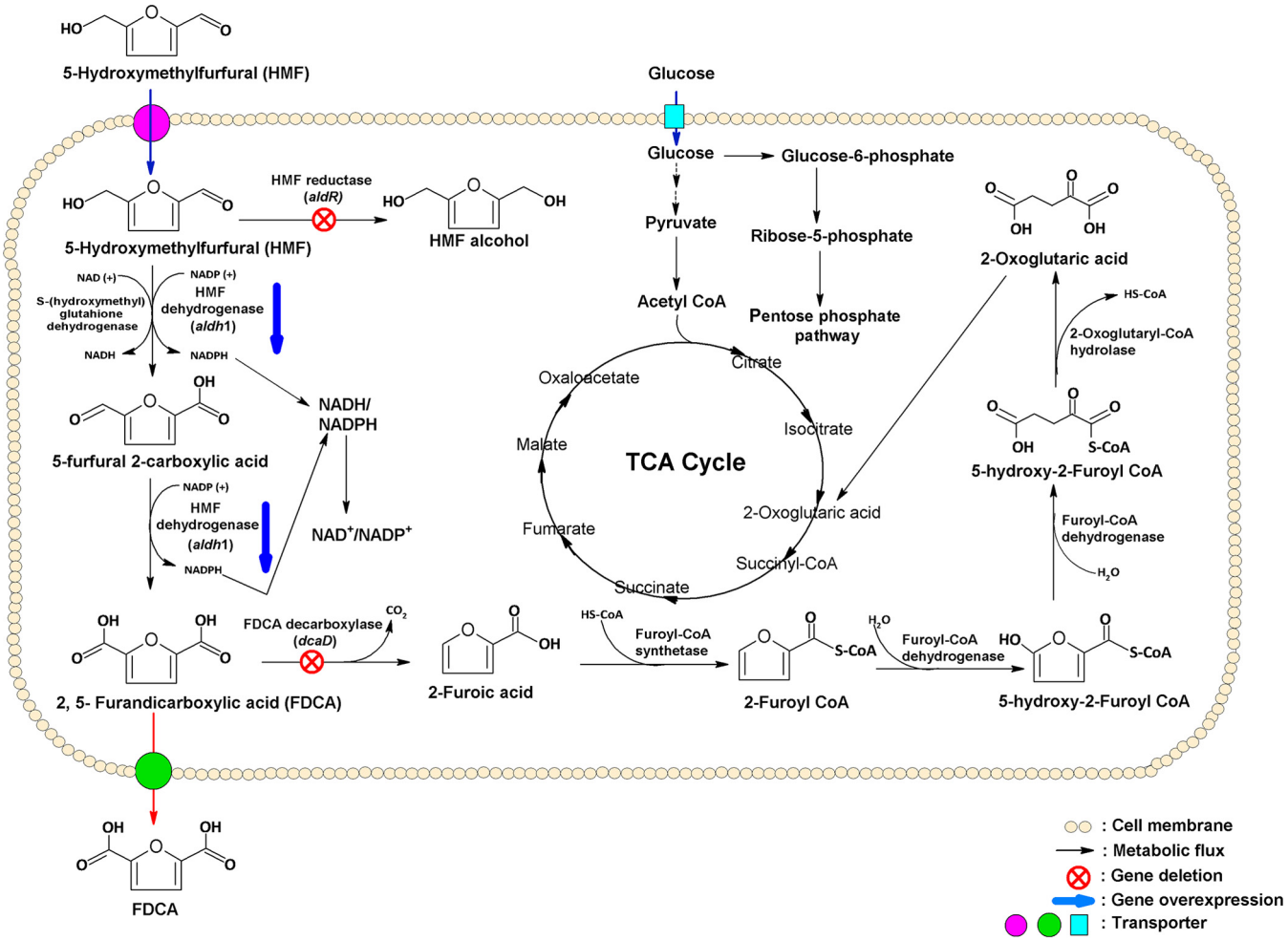

FIG 1 Metabolic pathway of 5-HMF and FDCA in *R. ornithinolytica* BF60. CoA, coenzyme A.

5-HMF production site (Suzhou Yake Chemical Reagent Co., Ltd.) contaminated with 5-HMF was inoculated into the LB medium supplemented with 30 mM 5-HMF and was incubated at 30°C for 3 days. Colonies showing better growth were inoculated into the liquid LB medium supplemented with 30 mM 5-HMF, and, after 48 h, the amount of FDCA was measured. One of the isolated strains, *R. ornithinolytica* BF60, which can effectively transform 5-HMF to FDCA (see Fig. S3A in the supplemental material), was identified by 16S rRNA sequence analysis and deposited at the China Center for Type Culture Collection (CCTCC) under accession number M2014391. The *R. ornithinolytica* BF60 strain was found to be a Gram-negative, oxidase-negative, aerobic, immotile, capsulated, and facultatively anaerobic bacterium. An image of strain *R. ornithinolytica* BF60 is shown in Fig. S3B. At the same time, we compared the capacity for FDCA production from 5-HMF with that of one standard *Raoultella* strain. *R. ornithinolytica* BF60 showed higher biotransformation ability than the standard *R. ornithinolytica* strain, ATCC 33257 (Fig. S4). Physiological and biochemical characterization procedures, performed at CCTCC, showed that the characteristics of *R. ornithinolytica* BF60 are strikingly similar to those of previously reported *Raoultella* strains (15, 16). The 16S rRNA sequence shows 99% identity with those of *Raoultella* and *Klebsiella* species. A phylogenetic tree of the 16S rRNAs from different strains was constructed using Molecular Evolutionary Genetics Analysis (MEGA 4.1) software and the neighbor-joining (NJ) method where repeated bootstrapping analyses were performed 1,000 times. The 16S rRNA from *R. ornithinolytica* BF60 was found to be the closest to the ortholog from *R. ornithinolytica* strain ATCC 19374T (Fig. S5). On the basis of these results, the isolated

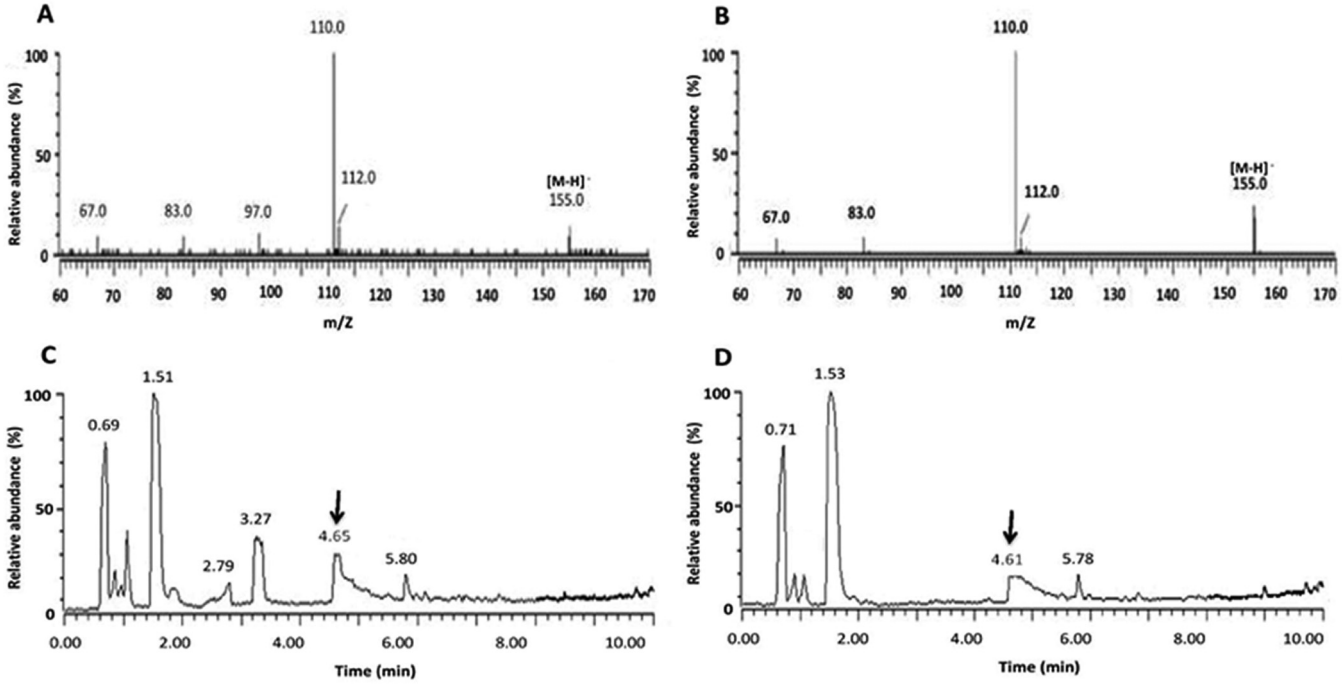

FIG 2 LC-MS analysis and UPLC-ESI-TOF-MS analysis of FDCA produced by *R. ornithinolytica* BF60 strains. (A) Selected-ion chromatogram analysis of FDCA (*m/z* 155.0 $[M - H]^-$) produced by the authentic FDCA standard. (B) Selected-ion chromatogram analysis of FDCA (*m/z* 155.0 $[M - H]^-$) produced by *R. ornithinolytica* BF60. (C) UPLC trace for authentic standard of FDCA (*Rt* = 4.65). (D) UPLC trace for FDCA produced by *R. ornithinolytica* BF60 (*Rt* = 4.61). *Rt*, retention time.

strain was classified as *R. ornithinolytica* BF60. As shown by mass spectrometric (MS) identification of samples isolated from the biotransformation buffer of the *R. ornithinolytica* BF60 strain, one compound had an *m/z* value of 155.0 [M − H] (Fig. 2B), which was confirmed by means of the FDCA standard (Fig. 2A). In addition, the compound had the same ultra-high-performance liquid chromatography (ultra-HPLC) trace as an authentic FDCA standard (Fig. 2C) and Fig. 2D shows the FDCA from *R. ornithinolytica*. These results confirmed that the *R. ornithinolytica* BF60 strain synthesizes FDCA.

Biochemical characterization of whole-cell biocatalyst and process optimization for FDCA production. An ideal whole-cell biocatalyst should be genetically amenable, grow fast in simple media, produce large amounts of the enzyme, and be compatible with subsequent downstream processing regimens (17). Thus, optimization of biochemical properties of the whole-cell biocatalyst for superior production is vital in whole-cell biotransformation processes. Therefore, the reaction conditions (e.g., pH, temperature, substrate concentration, and biocatalyst dose) were optimized. First, the optimal pH of the whole-cell biocatalyst was determined within a pH range of 6.0 to 10.0. The results revealed that the optimal pH was 8.0 (Fig. 3A) and that the biocatalyst retained more than 80% of its maximal activity between pH 7 and 9 (Fig. 3A). The optimal temperature of the whole-cell biocatalyst was then determined and found to be within the range of 20 to 45°C. The results showed that the whole-cell biocatalytic activity increased with increasing temperature from 20°C to 30°C and decreased beyond 35°C (Fig. 3B). The maximal activity of the recombinant biocatalyst was observed at 30°C, and the biocatalyst retained 80% of its maximal activity at 35°C (see Fig. 3B). At temperatures above 35°C, the biocatalytic activity decreased considerably, possibly because of the thermal deactivation of the relevant enzymes in the cells of *R. ornithinolytica* BF60 during the oxidation reaction. We next determined the optimal 5-HMF concentration by testing concentrations between 25 and 150 mM. FDCA production reached the highest level (12.08 μmol · liter^{-1} · h^{-1}) at 100 mM 5-HMF, indicating that substrate concentrations higher than 100 mM inhibit the reaction driven by the biocatalyst (Fig. 3C). The cell harvesting phase is the most significant part of the whole-cell bioconversion process because the enzymes involved in biotransformation

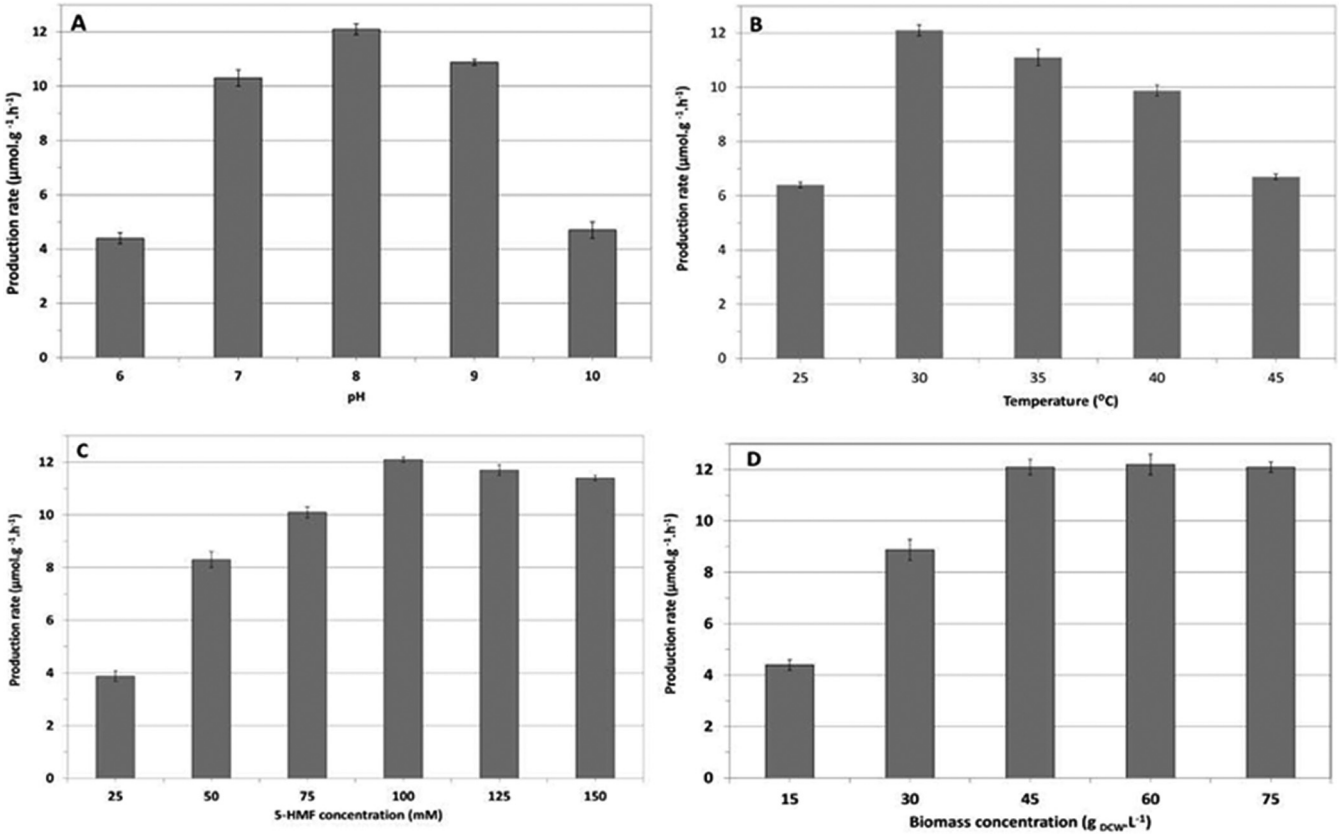

FIG 3 Influence of pH, temperature, substrate concentration, and cell concentration on whole-cell catalytic activity. (A) Influence of pH on the production rate. (B) Influence of temperature on the production rate. (C) Influence of substrate concentration on the production rate. (D) Effects of the biocatalyst concentration on the production rate. The data shown represent the averages ± standard deviations (SD) of results of three independent replicates.

are mostly produced during a specific phase. When the effect of the cell harvesting phase on the FDCA production rate was analyzed, we found that harvesting at the late exponential phase was the best for the biotransformation process (Table 1). In addition, it was observed that when 5-HMF was added at the biocatalyst preparation stage, the growth of the biocatalyst was greatly reduced due to its toxic effect on the *R. ornithinolytica* BF60 strain. To determine the optimal biocatalyst concentration for FDCA production, we performed the reactions with cell concentrations ranging from 15 to 75 g cells/liter. The FDCA production rate was the highest at 45 g cells/liter and did not increase at higher cell concentrations (Fig. 3D). Optimization of the biochemical characteristics by means of the fractional factorial design showed similar results (see Table S1 in the supplemental material). This finding suggests that high cell concentrations do not enhance FDCA production; perhaps O_2 becomes a limiting factor because the pathway generates reducing power which must be oxidized to sustain the flux.

TABLE 1 Effect of cell growth phase on FDCA production

Growth phase of *R. ornithinolytica* BF60[a]	Time since inoculation (h)	OD at 600 nm (±SD)	Production rate of FDCA (μmol · g^{-1} · h^{-1})
Early exponential	9	7 ± 1.2	5.93 ± 0.41
Mid-exponential	13	14 ± 1.4	9.57 ± 0.32
Late exponential	18	21 ± 0.7	12.05 ± 0.18
Early stationary	21	23 ± 0.9	10.23 ± 0.39
Late stationary	25	22 ± 1.1	4.35 ± 0.54

[a]Identical amounts of whole-cell biocatalyst were taken from cell suspensions of the corresponding phases, and reactions were performed for 6 h. Experiments were repeated three times. The starting OD during the inoculation was 0.05 at 600 nm.

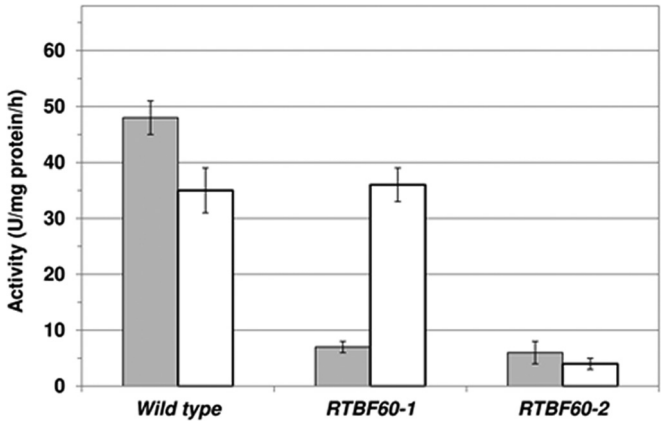

FIG 4 Activity of FDCA decarboxylase (gray bar) and 5-HMF reductase (white bar) in the wild-type strain, the dicarboxylic acid decarboxylase mutant (RTBF60-1), and the dicarboxylic acid decarboxylase and aldehyde reductase mutant (RTBF60-2). The data shown represent the averages ± SD of results of three independent replicates.

Effects of mutating the FDCA decarboxylase and aldehyde reductase genes on FDCA production. Because FDCA can be used by whole-cell biocatalysts, it was interesting to determine whether elimination of the FDCA degradation pathway improves FDCA production. In this study, we used the TargeTron mobile group II intron gene insertional mutagenesis system to create an insertional mutant of *dcaD*, the gene encoding dicarboxylic acid decarboxylase (RTBF60-1), and thereby to reduce FDCA degradation (18, 19). Successful insertion was confirmed by PCR with gene- and intron-specific primers and by Southern blotting (see Fig. S6 and S7 in the supplemental material). The insertional mutation of *dcaD* in *R. ornithinolytica* BF60 reduced the FDCA decarboxylase activity (Fig. 4). This gene shares a similarity with the genes in the *ubiD* family, which encode decarboxylase enzymes that catalyze conversion of 3-polyprenyl-4-hydroxybenzoate to 2-polyprenylphenol in the biosynthesis of ubiquinone. When we studied the time course of FDCA production from 5-HMF by the mutant, productivity reached 9.2 g/liter, and the biotransformation ratio increased to ~59% (Fig. 5A and B). In addition, during this reaction, 5-HMF is usually converted not only to its corresponding acid but also to the corresponding alcohol. Therefore, to

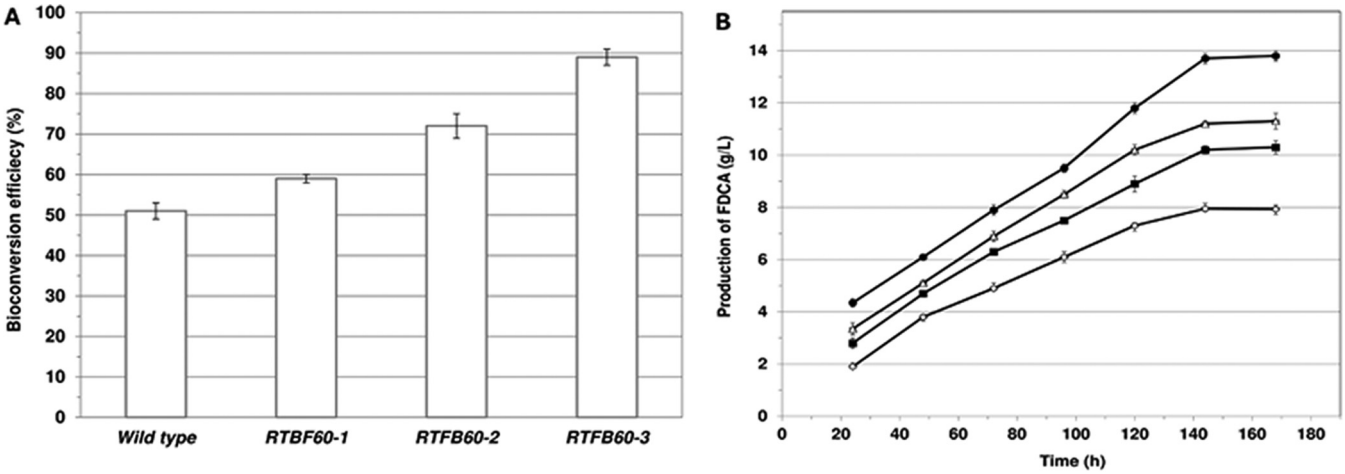

FIG 5 Effect of mutagenesis on the molar conversion efficiency and time profile for product formation. (A) Efficiency of conversion of different mutant and overexpressed strains from 5-HMF to FDCA production (mol/mol). (B) Time profile for the production of FDCA from 100 mM 5-HMF by different whole-cell biocatalysts. Wild type, ○; RTBF60-1, ■; RTBF60-2, Δ; RTBF60-3, ●. Data were analyzed using the Student *t* test. *P* values of less than 0.05 were considered statistically significant (the *P* value for comparisons of the wild type to the RTBF60-1 strain was 0.0004; the *P* value for comparisons of the wild type to the RTBF60-2 strain was 0.0002; and the *P* value for comparisons of the wild type to the RTBF60-3 strain was 0.0004). The data shown represent the averages ± SD of results of three independent replicates.

determine the proportion of 5-HMF converted to HMF alcohol, the amount of HMF alcohol in the reaction mixture was measured. We found that a substantial proportion (~15%) of 5-HMF was converted to HMF alcohol by aldehyde reductase. As a result, the remaining portion (~85%) of 5-HMF was converted to HMF acid and no 5-HMF was assimilated by the whole cells. Therefore, to decrease the aldehyde reductase activity and minimize substrate conversion to HMF alcohol, we mutated an aldehyde reductase gene (*aldR*) in the *R. ornithinolytica* BF60 mutant (RTBF60-1) strain. The resulting mutant showed lower 5-HMF reductase activity than the wild-type strain and RTBF60-1 did (Fig. 4); accordingly, as shown by mass balance analysis, no HMF was assimilated in that pathway. In the *R. ornithinolytica* BF60-2 double mutant, the 5-HMF conversion efficiency and FDCA titer reached 72% and 11.3 g/liter, respectively (Fig. 5B). These results indicate that, in the whole-cell biocatalyst, a portion of 5-HMF is converted to the corresponding alcohol and a portion of FDCA goes through the degradation pathway during the biotransformation process.

The effect of overexpressing the aldehyde dehydrogenase gene and the sequential feeding of 5-HMF on FDCA production. 5-HMF is usually oxidized to the corresponding monocarboxylic acid, which is further oxidized to FDCA by an oxidoreductase or dehydrogenase(s) (20). To increase FDCA production, three aldehyde dehydrogenase genes from *R. ornithinolytica* BF60 were cloned and overexpressed in the dicarboxylic acid decarboxylase and aldehyde reductase double insertional mutant. Among the three aldehyde dehydrogenase genes, only the gene encoding aldehyde dehydrogenase 1 showed ~23% higher production than the control (without overexpressing any aldehyde dehydrogenase enzyme) (see Fig. S8 in the supplemental material). The overexpression was verified with and without addition of isopropyl-β-D-1-thiogalactopyranoside (IPTG), and we found that the gene encoding aldehyde dehydrogenase 1 was overexpressed efficiently under the control of the T7 promoter (Fig. S9). Then, the enzyme kinetics of aldehyde dehydrogenase 1 were analyzed on two substrates, 5-HMF and FFCA. The K_m values for 5-HMF and FFCA were 11.2 $\pm$ 0.4 and 23.5 $\pm$ 0.3 mM, respectively, and the k_{cat}/K_m values for 5-HMF and FFCA were 5.1 and 1.7 $mM^{-1} \cdot min^{-1}$, respectively (see Table S2 in the supplemental material). Aldehyde dehydrogenase 1 oxidized 5-HMF to 5-formyl-2-furoic acid and FFCA to FDCA, although its affinity for 5-HMF was higher than that for FFCA. The aldehyde dehydrogenase 1-overexpressing strain (RTBF60-3) produced 13.9 g/liter FDCA compared to the 11.2 g/liter produced by the double insertional mutant RTBF60-2 (Fig. 5B). Moreover, HPLC analysis suggested that the amount of FFCA in the reaction medium had decreased significantly (Fig. S10). Therefore, due to aldehyde dehydrogenase 1 overexpression, reaction intermediates were efficiently converted to the product, thereby increasing the FDCA titer without accumulation of the intermediates in the biotransformation process. In addition, sequential feeding of 5-HMF (2.0 mM/h, for 50 h) was tried to test whether it could improve the production titer because the sequential feeding helps to start the biotransformation at a lower concentration of 5-HMF and to eliminate the toxic effects of the high substrate concentration at the start of the reaction process. The FDCA titer reached only 13.1 g/liter as a result of sequential feeding (Fig. S11).

DISCUSSION

In contrast to the fossil resources, renewable lignocellulosic biomass is an easily obtainable substrate (abundant as a feedstock) and its price is low also. First, we isolated and identified a new strain, *R. ornithinolytica* BF 60, that can efficiently produce FDCA from 5-HMF, which is a basic furanic compound, from biorenewable sources. It was recently reported that *Raoultella* species are members of lignocellulose-degrading communities and play an active role in the response to furanic compounds (21). For the production of fine chemicals and pharmaceutical compounds, whole-cell-based biotransformation processes have been developed through process optimization and engineering of cellular metabolic pathways (22, 23). Because the existing genetic engineering tools are inadequate for *R. ornithinolytica*, further genetic improvements have been a challenge. To overcome this obstacle, a gene insertional mutagenesis

system based on mobile group II intron technology was used here for *R. ornithinolytica* BF60 (24–28).

The furanic carboxylic acid compound was found to undergo facile decarboxylation by the aldehyde decarboxylase of various microorganisms. For example, in *Escherichia coli*, *ubiD* is involved in the decarboxylation of the metabolite 3-polyprenyl-4-hydroxybenzoate. The amino acid sequences of *dcaD* from *R. ornithinolytica* BF60 and *ubiD* from *E. coli* are 96% similar. The *hmfFG* genes in *C. basilensis* HMF14, which encode two putative decarboxylases of the *ubiD* type, are similar and operate in concert (29, 30). In addition, mutants with disrupted *hmfFG* genes accumulate HMF acid and FDCA when cultured in the presence of HMF, suggesting that the carboxylic acids are substrates of HmfFG (20). In the present study, a comparable phenomenon was observed in the dicarboxylic acid decarboxylase mutant (RTBF60-1): the decarboxylase activity was decreased whereas the accumulation of 2,5-FDCA increased to 9.2 from 7.9 g/liter (Fig. 4 and 5B).

Transformation of a toxic aldehyde compound into a less toxic alcohol is a common detoxification strategy in various microorganisms (31–34). Mostly, aldehyde reductases from various microbes, including *E. coli* and *Saccharomyces cerevisiae*, alleviate 5-HMF toxicity by catalyzing its NADPH-dependent conversion to the corresponding alcohol (35). In the present study, an enzyme (aldehyde reductase, encoded by *aldR*) was identified that reduced furfural toxicity by converting the relatively toxic furfural to a less toxic furfuryl alcohol. Typically, aldehyde reductase genes, as isolated from *S. cerevisiae* strain NRRL Y-12632 and *E. coli* strain LYO1, are also involved in the detoxification of furfural and 5-HMF (36, 37). In addition, in the ethanologenic *E. coli* LY180 strain, an aldehyde reductase (*yqhD*) gene was shown to have NADPH-dependent furfural reductase activity (38). In the case of *R. ornithinolytica* BF60, the identified aldehyde reductase gene is ~78% similar to *yqhD* of *E. coli* LY180 (see Table S4 in the supplemental material). In addition, in the *aldR* mutant of *R. ornithinolytica* BF60 (RTBF60-2), the substrate availability was increased and the FDCA production titer was also increased by 15% compared to the wild-type level (Fig. 5B).

On the other hand, aldehyde dehydrogenases or oxidases usually participate in the formation of a corresponding carboxylic acid in other microorganisms and are dependent on the presence of the cofactor NADPH for catalysis. During the enzymatic transformation, the use of cofactors in stoichiometric amounts is not only costly but also troublesome (39). Therefore, the use of a whole-cell biocatalyst for the biotransformation reaction is advantageous (40). However, after whole-cell biotransformation by the wild-type biocatalyst, FFCA was also detected in the reaction mixture with FDCA in our study (see Fig. S10A in the supplemental material). Therefore, we tested whether overexpression of aldehyde dehydrogenase 1 in the dicarboxylic acid decarboxylase and aldehyde reductase mutant (RTBF60-2) strain resulted in conversion of the remaining FFCA to FDCA. In addition, during the early reaction, oxidation of 5-HMF yielded 2,5-diformylfuran (DFF), suggesting that another alcohol dehydrogenase, specifically, a hydroxymethyl-type alcohol dehydrogenase, may be involved in the reaction and acts synergistically with aldehyde dehydrogenase 1 in the first oxidation of HMF to the HMF acid, thus increasing the overall efficiency of the biocatalyst. Because DFF was found to be converted into FFCA by carbonyl oxidation after its formation, FFCA and FDCA were the main products observed in the reaction mixture after the biotransformation reaction. Most of FFCA was converted to FDCA by the engineered biocatalyst RTBF60-3 overexpressing aldehyde dehydrogenase 1 (Fig. S10B); ultimately, the production titer of FDCA was increased to 13.9 from 11.2 g/liter (Fig. 5B). Therefore, the combination of expression of the gene encoding aldehyde dehydrogenase 1 and mutation of *dcaD* and *aldR* was required for the higher biotransformation efficiency. A similar outcome was observed when alcohol dehydrogenases (YneI and YdcW) were overexpressed in *Klebsiella pneumoniae* to improve the production of 3-hydroxypropionic acid (41). On the other hand, according to the results of the sequential feeding experiment, it can be concluded that the *R. ornithinolytica* whole-cell biocatalyst has the ability to overcome certain toxic effects of 5-HMF and that FDCA has no toxic effects. These data are in

TABLE 2 Strains and plasmids used in this study

Strain or plasmid	Characteristic(s)[a]	Source or reference
Strains		
Escherichia coli JM109	*recA1 endA1 gyrA96 thi hsdR17 supE44 relA1* Δ(*lac-proAB*)/F′ (*traD36 proAB*$^+$ *lacI*q *lacZ*ΔM15)	TaKaRa, Otsu, Japan
Escherichia coli BL21(DE3)	*fhuA2* [*lon*] *ompT gal* (λ *DE3*) [*dcm*] Δ*hsdS* λ *DE3* = λ sBamHIo ΔEcoRI-B *int*::(*lacI*::*PlacUV5*::*T7* gene 1) *i21* Δ*nin5*	Tiangen, China
R. ornithinolytica BF60	Wild type	This work
RTBF60-1	*R. ornithinolytica* BF60 derivate, insertional mutant in the *dcaD* gene encoding dicarboxylic acid decarboxylase	This work
RTBF60-2	RTBF60-1 derivate, insertional mutant in the *aldR* gene encoding aldehyde reductase	This work
RTBF60-3	RTBF60-2 derivate overexpressing the gene encoding aldehyde dehydrogenase 1 of *R. ornithinolytica* BF60	This work
RTBF60-4	RTBF60-2 derivate overexpressing the gene encoding aldehyde dehydrogenase 2 of *R. ornithinolytica* BF60	This work
RTBF60-5	RTBF60-2 derivate overexpressing the gene encoding aldehyde dehydrogenase 3 of *R. ornithinolytica* BF60	This work
R. ornithinolytica ATCC 31898	Wild type	ATCC
Plasmids		
pACD4K-C-loxP	Cm^r	Sigma-Aldrich, St. Louis, MO, USA
pAR1219	Amp^r	Sigma-Aldrich, St. Louis, MO, USA
pMD19T (Simple)	Amp^r	TaKaRa, Otsu, Japan
pTSC-repli	pTSC plasmid containing broad-host-range replicon of pBBR1	44
pBBR1MCS2	Kan^r	61

[a]Amp^r, ampicillin resistance; Ch^r, chloramphenicol resistance; Kan^r, kanamycin resistance.

agreement with a recent ecotoxicogenomic assessment, where researchers observed no toxicity associated with FDCA (42). However, the FDCA production approach described here has additional benefits with respect to the purification step. Highly purified FDCA could be obtained relatively easily by a mild purification method involving centrifugation and crystallization.

In conclusion, a powerful engineered whole-cell biocatalyst for the production of FDCA was constructed here by expressing an aldehyde dehydrogenase gene and mutating decarboxylase and aldehyde reductase genes in the newly isolated *R. ornithinolytica* BF60 strain. Because of the simplicity of the whole-cell biocatalytic procedure, our process is attractive in terms of expediency, productivity, and economy. Using the newly developed biocatalyst, we established an efficient process for one-step synthesis of FDCA, thus improving the multistep chemical process. The molar conversion ratio of 5-HMF is ~89%. Hence, the key challenge is to refine the transformation process to the point where biotransformation competes with the chemical synthesis as a method for production of FDCA. Overexpression of aldehyde dehydrogenase in *R. ornithinolytica* BF60 increased the FDCA yield and productivity and reduced the amount of intermediate products. Therefore, this overexpression also significantly improved FDCA purity, which will facilitate the downstream product separation process and will reduce the overall production cost. Novel strategies that target multidimensional regulation of metabolic networks are promising tools for optimization of cellular properties of microbial cell factories (43). Thus, our metabolically engineered strain holds promise for use in industrial fermentation for the production of FDCA, although further structural and process engineering may be necessary for economical production of FDCA of biological origin.

MATERIALS AND METHODS

Strains, vectors, and materials. The bacterial strains and plasmids used in this study are listed in Table 2. An EZ-10 Spin Column Plasmid MiniPrep kit, a DNA purification kit, restriction enzymes, and T4 DNA ligase were purchased from TaKaRa (Dalian, China). Other reagents as well as primer synthesis and DNA sequencing were provided by Shanghai Sangon Biological Engineering Technology and Services Co. Ltd. (Shanghai, China). Ampicillin, kanamycin, and chloramphenicol were purchased from Amresco

TABLE 3 Primers used in plasmid construction and in gene insertional mutant and 16S rRNA gene sequencing

Primer	Sequence[a]
Plasmid construction	
RtAldR_ F1	5′-ATGAAATACCACGATCTACGCGACTTTC-3′
RtAldR_R1	5′-TTATTTAAAGATAGCCAGCTCATCCCAG-3′
RtDcaD_F1	5′-ATGAACAATTTCGATCTACATACCCCAAC-3′
RtDcaD_R1	5′-TTAGCGTGCAGCCTCGTAAATCCGGCGGC-3′
RtAldh1_F1	5′-TCAGTAACGCACGCAGACCGATTTCGT-3′
RtAldh1 _R1	5′-ATGTCCACAGCACAGGTAGCGCTGCTT-3′
RtAldh1 _F2(HindIII)	5′-CCGAAGCTTATGTCCACAGCACAGGTAGCGCTGC-3′
RtAldh1 _R2(BamHI)	5′-CGCGGATCCTCAGTAACGCACGCAGACCGATTTC-3′
RtAldh2 _F1	5′-TTAAGACTGCAAATAGACGACCTGGGT-3′
RtAldh2 _R1	5′-ATGACAGCACCCGTTCAGCACCCGATG-3′
RtAldh2 _F2(HindIII)	5′-CCGAAGCTTATGACAGCACCCGTTCAGCACCCGA-3′
RtAldh2 _R2(BamHI)	5′-CGCGGATCCTTAAGACTGCAAATAGACGACCTGG-3′
RtAldh3 _F1	5′-ATGACAATAACCTGCAACTTATATACC-3′
RtAldh3 _R1	5′-TTAAAACGGCAGTTCGCGCGGACTGGT-3′
RtAldh3 _F2(HindIII)	5′-CCGAAGCTTATGACAATAACCTGCAACTTATATAC-3′
RtAldh3 _R2(BamHI)	5′-CGCGGATCCTTAAAACGGCAGTTCGCGCGGACTG-3′
RtAldh1 _F3(NcoI)	5′-CGCCCATGGCAATGTCCACAGCACAGGTAGCGCTGC-3′
RtAldh1 _R3(BamHI)	5′-CGCGGATCCGTAACGCACGCAGACCGATTTCGT-3′
pBBR1-F1	5′-GATCACCTAGGCTACAGCCGATAGTCTGGAACAGCGC-3′
pBBR1-R2	5′-AGATCAACTAGTGCCTCCGGCCTGCGGCCTGCGCGCTTCG-3′
Gene insertional mutant	
374|375s-IBS-*dcaD*	5′-AAAAAAGCTTATAATTATCCTTACCTGCCCGGCGCGTGCGCCCAGATAGGGTG-3′
374|375s-EBS1d-*dcaD*	5′-CAGATTGTACAAATGTGGTGATAACAGATAAGTCCGGCGCTCTAACTTACCTTTCTTTGT-3′
374|375s-EBS2-*dcaD*	5′-TGAACGCAAGTTTCTAATTTCGGTTGCAGGTCGATAGAGGAAAGTGTCT-3′
669|670s-IBS-*aldR*	5′-AAAAAAGCTTATAATTATCCTTAATTCTCCTGACCGTGCGCCCAGATAGGGTG-3′
669|670s-EBS1d-*aldR*	5′-CAGATTGTACAAATGTGGTGATAACAGATAAGTCCTGACCCTTAACTTACCTTTCTTTGT-3′
669|670s-EBS2-*aldR*	5′-TGAACGCAAGTTTCTAATTTCGGTTAGAATCCGATAGAGGAAAGTGTCT-3′
EBS Universal	5′-CGAAATTAGAAACTTGCGTTCAGTAAAC-3′
Con*dcaD*_F	5′-CAGGTACTGAACATGCCGACTAAGC-3′
Con*dcaD*_R	5′-CTTTCGTTTCGTTCCCATAGGTTCT-3′
Con*aldR*_F	5′-TCCAGGACCGCTTTGCCGAAGGCAT-3′
Con*aldR*_R	5′-GCTTTCGTTTCGTTCCCATAGGTTCT-3′
16S rRNA sequencing	
27F	5′-AGAGTTTGATCMTGGCTCAG-3′
1492R	5′-GGTTACCTTGTTACGACTT-3′

[a]Underlined sequences represent restriction enzyme sites.

(Solon, OH, USA), and isopropyl-β-D-1-thiogalactopyranoside (IPTG) was acquired from Merck (Darmstadt, Germany). 5-Hydroxymethylfurfural carboxylic acid was purchased from Matrix Scientific (Columbia, SC, USA) and 2,5-furandicarboxylic acid from Sigma-Aldrich (St. Louis, MO, USA). All other chemicals were commercially available reagents of analytical grade. *R. ornithinolytica* BF60 seed cultures were initiated in the Luria-Bertani (LB) medium, and whole-cell biocatalysts were grown in Terrific Broth.

Enrichment culture for isolation of microbes that produce FDCA from 5-HMF. Soil and water samples were collected from 5-HMF production sites (Suzhou Yake Chemical Reagent Company Limited, Suzhou Industrial Park) at Suzhou, Jiangsu, China. Bacteria were isolated from the samples using an enrichment technique. Ten grams of each sample was resuspended in 90 ml of sterile distilled water, and the suspensions were used as inocula for enrichment cultures. In the enrichment procedure, the LB medium (0.5% yeast extract, 1.0% peptone, 1.0% NaCl, pH 7.0) supplemented with 30 mM 5-HMF was used. Cultures in 100-ml flasks containing 20 ml of the medium were inoculated with 3 ml of a soil suspension, incubated with shaking at 200 rpm and 30°C, and then plated on LB agar plates. After incubation for 72 h at 30°C, morphologically different colonies were isolated and streaked on the same medium for further purification. *R. ornithinolytica* BF60 was found in the soil sample.

Morphological, physiological, and biochemical characterization of the transformed strains. The strain with the highest FDCA yield in preliminary experiments was selected. Its phenotypic and biochemical characteristics (e.g., Gram staining; motility; colony shape, size, and color on a nutrient agar plate; growth on MacConkey agar; catalase, oxidase, lipid, and starch hydrolysis) were determined by standard methods, according to *Bergey's Manual of Determinative Bacteriology* (45).

Phylogenetic analysis. Bacterial DNA was isolated from pure cultures, and almost the entire length of the 16S rRNA fragment was amplified by PCR using the universal primers 27F and 1492R (Table 3). The amplified 16S rRNA gene was purified from an agarose gel using a QIAquick gel extraction kit (Qiagen, Hilden, Germany) and was then ligated into a cloning vector (pMD19-T simple vector) using a cloning kit (Promega, Madison, WI, USA), and the resulting vector was transfected into JM109 cells. The recombinant plasmid was isolated, and cloning was confirmed by PCR. The insertion was then sequenced. The BLASTN

program (http://www.ncbi.nlm.nih.gov/BLAST/; NCBI, Bethesda, MD, USA) was used for homology searches with the default settings. Multiple alignments of the sequence were performed, and a neighbor-joining phylogenetic tree (46, 47) was constructed using ClustalW software (48).

Preparation of the whole-cell biocatalyst. For preparation of seed cultures, *R. ornithinolytica* BF60 cells were grown for 12 h at 30°C on a rotary shaker (200 rpm) in the LB medium without or with kanamycin (50 mg/liter) for the wild-type strain or mutant strains (and recombinant strains), respectively. The seed cultures (1% [vol/vol]) were then inoculated into Terrific Broth in a 3-liter vessel (BioFlo 115; New Brunswick Scientific Co., Edison, NJ, USA) with a working volume of 1.8 liters. The agitation speed, aeration rate, and temperature were maintained at 400 rpm, 1.0 volume per volume per min (vvm), and 30°C, respectively. After 20 h of incubation, the cells were harvested by centrifugation at 7,000 $\times$ *g* for 30 min at 4°C, and the pellets were washed twice with 50 mM phosphate buffer (pH 8.0). The cell pellet was then resuspended in the same buffer and kept at 4°C for further analyses. The biomass concentrations were measured spectrophotometrically (UV-2450 PC; Shimadzu Co., Kyoto, Japan) and converted to the dry cell weight (dcw) using the following equation: dcw (g/liter) = (0.44 $\times$ optical density at 600 nm [OD_{600}]) $-$ 0.02.

An assay of whole-cell biocatalytic activity. Erlenmeyer flasks (100 ml) were used for all reactions in which FDCA was produced. The reaction mixture (20 ml) was based on 50 mM phosphate buffer (pH 8.0). For assays of whole-cell biocatalytic activity, a mixture of 45.0 g/liter whole-cell biocatalyst and 100 mM 5-HMF was incubated on a rotary shaker at 220 rpm and 30°C for 24 h. The reaction was stopped by centrifugation at 10,000 $\times$ *g* for 10 min, and the supernatant was recovered for high-performance liquid chromatography (HPLC) quantification of FDCA, as described below.

Optimization of temperature, pH, and biocatalyst and substrate concentrations. All variables were optimized using 20 ml of a reaction mixture in a 100-ml Erlenmeyer flask. With the exception of the variables indicated below, reactions were carried out using the standard whole-cell biocatalytic reaction conditions described above. To optimize the temperature, the reaction was run at pH 8.0 and 220 rpm with temperatures ranging between 20°C and 60°C. For pH optimization, the conditions were 30°C, 220 rpm, Na_2HPO_4-KH_2PO_4 buffer (pH 6 to 9), and Tris-HCl buffer (pH 10). For optimization of the whole-cell biocatalyst concentration, the conditions were 30°C, 220 rpm, pH 8.0, and a cell concentration between 10 and 60 g/liter. For optimization of substrate concentration, the conditions were 30°C, 220 rpm, pH 8.0, and a 5-HMF concentration between 25 and 150 mM. The reactions were stopped by centrifugation at 10,000 $\times$ *g* for 10 min, and the supernatant was recovered for HPLC quantification of FDCA.

Optimization of the FDCA production by means of the fractional factorial design. A fractional factorial experimental design was implemented to further evaluate the effects of strain engineering and to choose the optimum values of pH (P), temperature (T), substrate concentration (S), and biomass concentration (M) for the conversion of HMF to HDCA. Each factor was verified at three levels in duplicate. Using the formula k^{n-1}, where k = level and n = number of factors, 27 experiments were executed in duplicate, and the average values were noted. The levels of pH were 7.0, 8.0, and 9.0; temperatures were 25°C, 30°C, and 35°C; substrate concentrations were 75, 100, and 125 mM; and biomass concentrations were 30, 45, and 60 g_{dcw}/liter. The fractional factorial design matrix showing the variables is presented in Table S1. To identify the process variables that have a significant effect on the response (i.e., $P < 0.05$), linear regression and analysis of variance were conducted and a regression relation between the process variables and the response variable was subsequently established. All statistical analyses were performed using Microsoft Excel 2010 software. The following second-order polynomial function was used to predict the optimum conditions: $Y = \beta_0 + \Sigma\beta_i X_i + \Sigma\beta_{i\ i} X^2 + \Sigma\beta_{i\ j} X_i X_j$ (where Y is the predicted response, X_i and X_j are the independent variables, and β_0, β_i, β_{ii}, and β_{ij} denote the intercept, linear, quadratic, and cross-product (interaction) coefficients, respectively.

Analysis of FDCA with HPLC and liquid chromatography with tandem mass spectrometry (LC-MS/MS). The amount of FDCA in the reaction mixture was determined by HPLC (1260 series; Agilent, Santa Clara, CA, USA) on an Aminex HPX-87H column (Bio-Rad, Torrance, CA, USA) at 40°C, with elution performed by the use of 5 mM H_2SO_4 at 0.5 ml/min and detection performed with a UV detector at a fixed wavelength of 230 nm. The HPLC retention time values of the standards of FDCA and FFCA were 20 min and 28 min, respectively. LC-MS/MS analysis of FDCA was performed using a Waters Acquity ultraperformance liquid chromatography (UPLC) apparatus connected to a photodiode array (PDA) detector and a matrix-assisted laser desorption ionization (MALDI) SYNAPT quadrupole-time of flight (Q-TOF) mass spectrometer (Waters, Milford, MA, USA), which was operated in negative electrospray ionization (ESI) mode. An Acquity UPLC CSH C_{18} column (Waters) (2.1 by 50 mm, 1.7-μm pore size) was used. The injection volume was 1 μl, and the column temperature was maintained at 45°C. As the mobile phase, buffer A (acetonitrile) and buffer B (ultrapure water/formic acid, 1,000:1 [vol/vol]) were used at a flow rate of 0.3 ml $\cdot$ min^{-1}. At the starting point, the flow consisted of 100% buffer B; buffer A was then increased to 10% over the next 3 min and to 100% over another 3 min. After 1 min of 100% buffer A treatment, the eluent was returned to 100% buffer B within 0.1 min, and the column was conditioned for 1.9 min before the next injection. The MS/MS operating conditions were as follows: source block temperature, 100°C; desolvation temperature, 400°C; desolvation gas flow, 500 liters/h; cone gas flow, 50 liters/h; cone voltage, 30 V; collision energy, 6 eV; capillary voltage, 3.0 kV; detector voltage, 1,900 V. The mass spectrometer scanned the data from 50 to 1,000 *m/z*. Data were acquired using Mass Lynx software, v.4.1 (Waters).

Measurement of HMF and HMF alcohol concentrations. HMF was quantified by a spectroscopic method (49). First, 1 ml of the reaction solution was centrifuged, and the supernatant was diluted with Milli-Q water to obtain a reaction solution of 5.0 ml after addition of 50 μl of Carrez solution I and 50 μl of Carrez solution II (50). After that, the reaction mixture was filtered. Aliquots of 0.5 ml

were placed into two tubes; 0.5 ml of deionized water was added to one tube and 0.5 ml of 0.2% sodium bisulfite solution was added to the second tube as a reference solution. The absorbance of the aqueous reaction solution at 284 nm was determined versus that of the reference solution, in order to avoid interference from other components at that wavelength. The absorbance at 336 nm was also determined to subtract the background absorbance. The HMF was quantified (in micrograms per liter) by means of the following formula:

$$\mathrm{HMF} = \left(A_{284} - A_{336}\right) \times 149.7 \times 5/W \quad (1)$$

where W is the weight of the sample and the factor 149.7 is a theoretical value linked to the molar extinction coefficient of HMF at 284 nm, which is 16,830 (51). Efficiency of conversion (C) of HMF was calculated by the following formula: $C = (M_1 - M_2/M_1) \times 100$ (where M_1 is the initial HMF concentration and M_2 the final HMF concentration). For assessment of conversion efficiency, the final time point was the time at which the reaction process was stopped (after 144 h) via separation of the whole-cell biocatalyst from the reaction mixture. HMF alcohol was quantified by HPLC (Agilent 1260 series; Santa Clara, CA, USA) on an Aminex HPX-87H column (Bio-Rad, Torrance, CA, USA) at 50°C, with elution by means of 5 mM H_2SO_4 at 0.6 ml/min and with detection using a refractive index detector.

Construction of a double gene insertional mutant of *R. ornithinolytica* BF60 and measurement of enzymatic activity. Mobile group II intron (TargeTron)-based genetic engineering systems have been used in investigations of many other bacterial species. The intron fragment is easily modified because the gene targeting specificity is determined solely by base pairing between the intron RNA and the targeted chromosomal DNA. The insertion can be targeted to any DNA sequence (52). Intron insertion into the chromosome involves a single-step transformation procedure with high efficiency. It is a promising approach to markerless mutagenesis, with consecutive introduction of several mutations into a single strain through curing of the donor plasmid (53, 54).

A double gene insertional mutant was constructed via intron insertion into the genome. First, the genes were amplified by degenerate PCR using oligonucleotides shown in Table 3. Primer sequences from *R. ornithinolytica* TNT (55) were used to obtain the native sequences of *R. ornithinolytica* BF60, and the native gene sequences were used for insertional mutagenesis experiments according to the TargeTron mutagenesis (Invitrogen, Carlsbad, CA, USA) protocol. First, the intron sequences were amplified by PCR from genomic DNA. Then, the amplicons were purified, digested with BsrGI and HindIII, and ligated with the pACD4K-C-loXp TargeTron plasmid (Fig. S2). *E. coli* JM109 cells were transformed with the TargeTron plasmids. Plasmids isolated from correct clones were transfected into *R. ornithinolytica* BF60 by electroporation.

Briefly, the laboratory stocks of *R. ornithinolytica* BF60 carrying the pAR1219 helper plasmid were inoculated into the LB medium containing 100 μg/ml ampicillin in a 1% inoculation ratio (for the overnight saturated culture) and grown aerobically at 30°C until the optical density (OD) of the culture at 600 nm reached 0.6 to 0.8. The cells were then harvested by centrifugation at 9,000 rpm for 20 min at 4°C. The cell pellet was washed with 1 volume of ice-cold 5 mM HEPES buffer and centrifuged at 9,000 rpm for 20 min at 4°C. The resulting cell pellet was resuspended in a 5% volume of ice-cold 10 mM HEPES buffer and used immediately for electroporation.

For each transformation procedure, 400 μl of a suspension of electrocompetent *R. ornithinolytica* BF60 cells was mixed with 1.0 μg of plasmid DNA and then placed in a 0.2-cm-gap-width precooled electroporation cuvette and incubated on ice for 10 min. A Gene Pulser Xcell electroporation system (Bio-Rad, Hercules, CA, USA) was connected to the chamber. Electroporation was carried out under the following conditions: voltage, 2,500 V; capacitance, 25 μF; resistance, 200 Ω. Next, the cuvette was placed on ice for 10 min. The cells were then transferred to 1 ml of the LB medium containing 1% glucose and grown at 30°C with shaking for 1 h. Thereafter, 100 μl of the transformation reaction was added to 3 ml of LB containing 25 μg/ml chloramphenicol and 1% glucose and incubated overnight at 30°C with shaking. After that, 40 μl of the overnight culture was added to 2 ml of LB broth containing 25 μg/ml chloramphenicol and 1% glucose. The culture was grown at 30°C to an OD_{600} of approximately 0.2, at which point the culture was cooled to 25°C in an incubator, supplemented with 10 μl of 100 mM IPTG, and incubated for an additional 30 min with shaking. The cells were immediately centrifuged at maximum speed in a microcentrifuge for 1 min. Then, the cells were resuspended in 1.0 ml of LB broth containing 1% glucose and incubated at 30°C for 1 h with shaking. Finally, 100 μl of the culture was plated on an LB agar plate containing 25 μg/ml kanamycin and grown overnight at 30°C for 3 to 4 days. Kanamycin-resistant colonies were picked for colony PCR to confirm the intron insertions by junction PCR, using one primer flanking the gene site and another inside the intron. First, the dicarboxylic acid decarboxylase (*dcaD*) enzyme was targeted for chromosomal insertion. Successful insertion was confirmed by PCR using gene- and intron-specific primers. The kanamycin resistance marker (used to select for the insertion) was removed via Cre-loxP-mediated recombination (56, 57) by means of a pTSC plasmid containing the broad-host-range replicon of pBBR1 (44). After that, the temperature-sensitive plasmid was expelled by incubation of the cells at 50°C for 12 h. After removal of the kanamycin resistance marker, the appropriate intron sequence was inserted into the alcohol reductase (*aldR*) gene (58), and the resistance marker was removed accordingly.

Southern blot analyses of the insertional mutant strains. Total genomic DNA was isolated from insertional mutant strains using an E.Z.N.A. bacterial genome extraction kit (Omega Bio-Tek Inc., Norcross, GA, USA). The total genomic DNA was digested overnight with the AvaI restriction endonuclease at 37°C; then, DNA fragments in the digests were separated by electrophoresis in a 0.8% agarose gel. After that, the DNA fragments were denatured and neutralized. Next, they were transferred to a nylon membrane (positively charged) for fixing by the standard method (Hybond-N^+; Amersham Biosciences, Ltd., UK). The

intron DNA fragment served as a hybridization probe that was prepared by PCR from the purified recombinant plasmid. Probe labeling and hybridization were performed using digoxigenin (DIG) High-Prime DNA labeling and detection starter kit I and an antidigoxigenin antibody conjugated with alkaline phosphatase (Roche Applied Science).

Construction of a vector for overexpression of the aldehyde dehydrogenase gene. Because pBBR1MCS-2 is a broad-host-range vector for Gram-negative bacteria, it was used to construct the recombinant vectors for overexpression of three native genes expressing aldehyde dehydrogenases in *R. ornithinolytica* BF60 by adding *lac* or T7 promoter at a SalI restriction site (Table S3) of pBBR1MCS2 and by transfection of the pAR1219 helper plasmid (which expresses T7 RNA polymerase under the control of the IPTG-inducible lac UV51 promoter) before transfection of the pBBR1MCS2 vector. For construction of the recombinant plasmid, first, the genes were amplified by degenerate PCR using oligonucleotides shown in Table 3 (derived from the sequences of *R. ornithinolytica* TNT) (55). The amplified fragments of genes were purified and ligated to a pMD19 simpleT vector. Next, the resulting plasmids were transfected into *E. coli*, and the recombinant plasmid was then purified and sequenced to verify the native gene sequences of *R. ornithinolytica* BF60. After that, the genes were again amplified using primers containing restriction enzyme digestion sites (Table 3). The amplicons were purified and digested with the corresponding enzymes. Next, the digested fragments were ligated to pET28a and pBBR1MCS-2 vectors and transfected into *E. coli* BL21(DE3) and double mutant *R. ornithinolytica* BF60 (RTBF60-2) strains, respectively. The recombinant constructs were confirmed by restriction analysis and verified by DNA sequencing.

Aldehyde dehydrogenase, aldehyde reductase, and decarboxylase activity assays. Cultures of the recombinant strains were centrifuged at 8,000 × *g* for 10 min, and the supernatants were used to assess the extracellular enzymatic activity. A cell pellet from 500 ml of the bacterial culture was resuspended in 20 ml of lysis buffer A, consisting of 50 mM Tris-HCl buffer (pH 8.0), 1 mM phenylmethanesulfonyl fluoride, 1 mM EDTA, and 1 mM dithiothreitol, and was ultrasonicated for 40 min on ice (cycles of 1-s sonication and 2-s pause) by means of a Vibra-Cell sonicator (Sonics, Newtown, CT, USA). The resulting lysate was centrifuged at a high speed (11,000 × *g*, 8 min, 4°C) to remove unbroken cells, and the supernatant was used for purification of aldehyde dehydrogenases for kinetic analysis. Proteins were purified to homogeneity in one step on a nickel-nitrilotriacetic acid (Ni-NTA) affinity column. The aldehyde dehydrogenase activity was assayed spectrophotometrically at 30°C by measuring the absorbance at 340 nm (NADH formation) in a mixture (1 ml) that consisted of 10 mM 5-HMF, 2.5 mM NAD, and 50 mM phosphate buffer (pH 8.0). The kinetic analyses were performed at six concentrations of substrates (5 to 40 mM). The initial velocities obtained during the first 5 min of a reaction were determined. The K_m, k_{cat}, and V_{max} values were obtained by linear regression analysis of the data plotted according to the method of Lineweaver and Burk. The concentration of the protein in the cell extracts and purified preparations was determined by the method of Lowry et al. (59) as modified by Bensadoun and Weinstein (60) to avoid EDTA interference.

Cell lysates were used for the assays of aldehyde reductase and decarboxylase activities. Aldehyde reductase activity was monitored by means of NADPH on a spectrophotometer by measuring the decrease in absorbance at 340 nm. The assays were carried out in 2.0-ml volumes at 30°C and lasted for 10 min. The reaction mixture consisted of 10 mM HMF–100 μM cofactor–50 mM potassium phosphate buffer (pH 7.0). Then, a crude cell extract was added to initiate a reaction. Using the reaction mixture as stated above without the lysates, we measured the blank sample on the spectrophotometer before each assay. Decarboxylase activity was measured as described previously (20). The reaction mixture consisted of 10 mM FDCA–50 μM pyridoxal 5′ phosphate–100 mM potassium phosphate buffer (pH 7.0). The crude cell extract was added to initiate the reaction. Samples were taken at certain intervals and analyzed by HPLC. The reaction was stopped by addition of HCl to the reaction mixture to reach the final concentration of 1 M. One unit of enzymatic activity was defined as the amount of protein that catalyzed production of 1 μM product from 10 mM substrate (FDCA or 5-HMF)–50 mM phosphate buffer (pH 8.0) at 30°C. All reagents were maintained in a 30°C water bath prior to use. All assays were performed three times.

Statistical analysis. All experiments were performed at least three times, and the results were expressed as means ± standard deviations ($n = 3$).

Accession number(s). *R. ornithinolytica* strain BF60 was deposited at the China Center for Type Culture Collection (CCTCC) under accession number M2014391 (http://www.cctcc.org/sci/microbe_common/searchc.php).

SUPPLEMENTAL MATERIAL

Supplemental material for this article may be found at https://doi.org/10.1128/AEM.02312-16.

TEXT S1, PDF file, 0.7 MB.

ACKNOWLEDGMENTS

This work was supported by the Priority Academic Program Development of Jiangsu Higher Education Institutions, the 111 Project (no. 111-2-06), and the Jiangsu province "Collaborative Innovation Center for Advanced Industrial Fermentation" industry development program.

REFERENCES

1. Fittig R, Heinzelmann H. 1876. Production of 2,5-furandicarboxylic acid by the reaction of fuming hydrobromic acid with mucic acid under pressure. Chem Ber 9:1198.
2. Gandini A. 2011. The irruption of polymers from renewable resources on the scene of macromolecular science and technology. Green Chem 13:1061–1083. https://doi.org/10.1039/c0gc00789g.
3. Gandini A, Silvestre AJD, Pascoalneto C, Sousa AF, Gomes M. 2009. The furan counterpart of poly(ethylene terephthalate): an alternative material based on renewable resources. J Polym Sci Part A Polym Chem 47:295–298. https://doi.org/10.1002/pola.23130.
4. Duennenberger M, Schellenbaum M. 1973. Swiss patent CH532890. Chem Abstr 78:159405t.
5. Lewkowski J. 2005. Synthesis, chemistry and applications of 5-hydroxymethylfurfural and its derivatives. Arch Org Che 2001:17–54.
6. Werpy T, Petersen G. 2004. Top value added chemicals from biomass. Volume I—results of screening for potential candidates from sugars and synthesis, gas. U.S. Department of Energy Efficiency and Renewable Energy. http://www.nrel.gov/docs/fy04osti/35523.pdf.
7. Zhou L, He Y, Ma Z, Liang R, Wu T, Wu Y. 2015. One-step degradation of cellulose to hydroxymethylfurfural in ionic liquid under mild conditions. Carbohydr Polym 117:694–700. https://doi.org/10.1016/j.carbpol.2014.10.062.
8. Yi G, Teong SP, Li X, Zhang Y. 2014. Purification of biomass-derived 5-hydroxymethylfurfural and its catalytic conversion to 2,5-furandicarboxylic acid. ChemSusChem 7:2131–2135. https://doi.org/10.1002/cssc.201402105.
9. Villa A, Schiavoni M, Campisi S, Veith GM, Prati L. 2013. Pd-modified Au on carbon as an effective and durable catalyst for the direct oxidation of HMF to 2,5-furandicarboxylic acid. ChemSusChem 6:609–612. https://doi.org/10.1002/cssc.201200778.
10. Casanova O, Iborra S, Corma A. 2009. Biomass into chemicals: aerobic oxidation of 5-hydroxymethyl-2-furfural into 2,5-furandicarboxylic acid with gold nanoparticle catalysts. ChemSusChem 2:1138–1144. https://doi.org/10.1002/cssc.200900137.
11. Wierckx N, Koopman F, Ruijssenaars HJ, de Winde JH. 2011. Microbial degradation of furanic compounds: biochemistry, genetics, and impact. Appl Microbiol Biotechnol 92:1095–1105. https://doi.org/10.1007/s00253-011-3632-5.
12. Koopman F, Wierckx N, de Winde JH, Ruijssenaars HJ. 2010. Efficient whole-cell biotransformation of 5-(hydroxymethyl)furfural into FDCA, 2,5-furandicarboxylic acid. Bioresour Technol 101:6291.
13. Triebl C, Nikolakisb V, Ierapetritou M. 2013. Simulation and economic analysis of 5 hydroxymethylfurfural conversion to 2,5-furandicarboxylic acid. Comput Chem Eng 52:26–34. https://doi.org/10.1016/j.compchemeng.2012.12.005.
14. Schicklberger M, Shapiro N, Loqué D, Woyke T, Chakraborty R. 2015. Draft genome sequence of *Raoultella terrigena* R1Gly, a diazotrophic endophyte. Genome Announc 3:e00607-15. https://doi.org/10.1128/genomeA.00607-15.
15. Drancourt M, Bollet C, Carta A, Rousselier P. 2001. Phylogenetic analyses of *Klebsiella* species delineate *Klebsiella* and *Raoultella* gen. nov., with description of *Raoultella ornithinolytica* comb. nov., *Raoultella terrigena* comb. nov., and *Raoultella planticola* comb. nov. Int J Syst Evol Microbiol 51:925–932. https://doi.org/10.1099/00207713-51-3-925.
16. Izard D, Ferragut C, Gavini F, Kersters K, de Ley J, Leclerc H. 1981. *Klebsiella terrigena*, a new species from soil and water. Int J Syst Bact 31:116–127. https://doi.org/10.1099/00207713-31-2-116.
17. Klatte S, Lorenz E, Wendisch VF. 2014. Whole cell biotransformation for reductive amination reactions. Bioengineered 5:56–62. https://doi.org/10.4161/bioe.27151.
18. Rodriguez SA, Davis G, Klose KE. 2009. Targeted gene disruption in *Francisella tularensis* by group II introns. Methods 49:270–274. https://doi.org/10.1016/j.ymeth.2009.04.011.
19. Wang Y, Li X, Milne CB, Janssen H, Lin W, Phan G, Hu H, Jin YS, Price ND, Blaschek HP. 2013. Development of a gene knockout system using mobile group II introns (Targetron) and genetic disruption of acid production pathways *in Clostridium beijerinckii*. Appl Environ Microbiol 79:5853–5863. https://doi.org/10.1128/AEM.00971-13.
20. Koopman F, Wierckx N, de Winde JH, Ruijssenaars HJ. 2010. Identification and characterization of the furfural and 5-(hydroxymethyl)furfural degradation pathways of Cupriavidus basilensis HMF14. Proc Natl Acad Sci U S A 107:4919–4924.
21. Jiménez DJ, Korenblum E, van Elsas JD. 2014. Novel multispecies microbial consortia involved in lignocellulose and 5-hydroxymethylfurfural bioconversion. Appl Microbiol Biotechnol 98:2789–2803. https://doi.org/10.1007/s00253-013-5253-7.
22. Ishige T, Honda K, Shimizu S. 2005. Whole organism biocatalysis. Curr Opin Chem Biol 9:174–180. https://doi.org/10.1016/j.cbpa.2005.02.001.
23. Panke S, Wubbolts M. 2005. Advances in biocatalytic synthesis of pharmaceutical intermediates. Curr Opin Chem Biol 9:188–194. https://doi.org/10.1016/j.cbpa.2005.02.007.
24. Frazier CL, San Filippo J, Lambowitz AM, Mills DA. 2003. Genetic manipulation of *Lactococcus lactis* by using targeted group II introns: generation of stable insertions without selection. Appl Environ Microbiol 69:1121–1128. https://doi.org/10.1128/AEM.69.2.1121-1128.2003.
25. Karberg M, Guo HT, Zhong J, Coon R, Perutka J, Lambowitz AM. 2001. Group II introns as controllable gene targeting vectors for genetic manipulation of bacteria. Nat Biotechnol 19:1162–1167. https://doi.org/10.1038/nbt1201-1162.
26. Shao L, Hu S, Yang Y, Gu Y, Chen J, Jiang W, Yang S. 2007. Targeted gene disruption by use of a group II intron (targetron) vector in *Clostridium acetobutylicum*. Cell Res 17:963–965. https://doi.org/10.1038/cr.2007.91.
27. Chen Y, McClane BA, Fisher DJ, Rood JI, Gupta P. 2005. Construction of an alpha toxin gene knockout mutant of *Clostridium perfringens* type A by use of a mobile group II intron. Appl Environ Microbiol 71:7542–7547. https://doi.org/10.1128/AEM.71.11.7542-7547.2005.
28. Tolonen AC, Chilaka AC, Church GM. 2009. Targeted gene inactivation in *Clostridium phytofermentans* shows that cellulose degradation requires the family 9 hydrolase Cphy3367. Mol Microbiol 74:1300–1313. https://doi.org/10.1111/j.1365-2958.2009.06890.x.
29. Gulmezian M, Hyman KR, Marbois BN, Clarke CF, Javor GT. 2007. The role of UbiX in *Escherichia coli* coenzyme Q biosynthesis. Arch Biochem Biophys 467:144–153. https://doi.org/10.1016/j.abb.2007.08.009.
30. Howlett BJ, Bar-Tana J. 1980. Polyprenyl p-hydroxybenzoate carboxylase in flagellation of Salmonella typhimurium. J Bacteriol 143:644–651.
31. Petersson A, Almeida JRM, Modig T, Karhumaa K, Hahn-Hägerdal B, Gorwa-Grauslund MF, Lidén G. 2006. A 5-hydroxymethyl furfural reducing enzyme encoded by the *Saccharomyces cerevisiae* ADH6 gene conveys HMF tolerance. Yeast 23:455–464. https://doi.org/10.1002/yea.1370.
32. Laadan B, Almeida JR, Rådström P, Hahn-Hägerdal B, Gorwa-Grauslund M. 2008. Identification of an NADH-dependent 5-hydroxymethylfurfural-reducing alcohol dehydrogenase in *Saccharomyces cerevisiae*. Yeast 25:191–198. https://doi.org/10.1002/yea.1578.
33. Heer D, Heine D, Sauer U. 2009. Resistance of Saccharomyces cerevisiae to high concentrations of furfural is based on NADPH-dependent reduction by at least two oxireductases. Appl Environ Microbiol 75:7631–7638. https://doi.org/10.1128/AEM.01649-09.
34. Liu ZL, Moon J, Andersh BJ, Slininger PJ, Weber S. 2008. Multiple gene-mediated NAD (P) dependent aldehyde reduction is a mechanism of in situ detoxification of furfural and 5-hydroxymethylfurfural by *Saccharomyces cerevisiae*. Appl Microbiol Biotechnol 81:743–753. https://doi.org/10.1007/s00253-008-1702-0.
35. Jordan DB, Braker JD, Bowman MJ, Vermillion KE, Moon J, Liu ZL. 2011. Kinetic mechanism of an aldehyde reductase of *Saccharomyces cerevisiae* that relieves toxicity of furfural and 5 hydroxymethylfurfural. Biochim Biophys Acta 1814:1686–1694. https://doi.org/10.1016/j.bbapap.2011.08.011.
36. Liu ZL, Moon J. 2009. A novel NADPH-dependent aldehyde reductase gene from Saccharomyces cerevisiae NRRL Y-12632 involved in the detoxification of aldehyde inhibitors derived from lignocellulosic biomass conversion. Gene 446:1–10. https://doi.org/10.1016/j.gene.2009.06.018.
37. Gutiérrez T, Ingram LO, Preston JF. 2006. Purification and characterization of a furfural reductase (FFR) from *Escherichia coli* strain LYO1—an enzyme important in the detoxification of furfural during ethanol production. J Biotechnol 121:154–164. https://doi.org/10.1016/j.jbiotec.2005.07.003.
38. Miller EN, Jarboe LR, Yomano LP, York SW, Shanmugam KT, Ingram LO. 2009. Silencing of NADPH-dependent oxidoreductase genes (*yqhD* and

dkgA) in furfural-resistant ethanologenic *Escherichia coli*. Appl Environ Microbiol 75:4315–4323. https://doi.org/10.1128/AEM.00567-09.
39. Macleod SM, Stickler DJ. 2007. Species interactions in mixed-community crystalline biofilms on urinary catheters. J Med Microbiol 56:1549–1557. https://doi.org/10.1099/jmm.0.47395-0.
40. Duetz WA, van Beilen JB, Witholt B. 2001. Using proteins in their natural environment: potential and limitations of microbial whole-cell hydroxylations in applied biocatalysis. Curr Opin Biotechnol 12:419–425. https://doi.org/10.1016/S0958-1669(00)00237-8.
41. Luo LH, Seo JW, Heo SY, Oh BR, Kim DH, Kim CH. 2013. Identification and characterization of *Klebsiella pneumoniae* aldehyde dehydrogenases increasing production of 3-hydroxypropionic acid from glycerol. Bioprocess Biosyst Eng 36:1319–1326. https://doi.org/10.1007/s00449-012-0880-4.
42. Chen GM, van Straalena N, Roelofsa D. 27 May 2016. The ecotoxicogenomic assessment of soil toxicity associated with the production chain of 2,5-furandicarboxylic acid (FDCA), a candidate bio-based green chemical building block. Green Chem https://doi.org/10.1039/C6GC00430J.
43. Robitaille AM, Christen S, Shimobayashi M, Cornu M, Fava LL, Moes S, Prescianotto-Baschong C, Sauer U, Jenoe P, Hall MN. 2013. Quantitative phosphoproteomics reveal mTORC1 activates de novo pyrimidine synthesis. Science 339:1320–1323. https://doi.org/10.1126/science.1228771.
44. Yan X, Yu HJ, Hong Q, Li SP. 2008. Cre/lox system and PCR-based genome engineering in Bacillus subtilis. Appl Environ Microbiol 74:5556–5562. https://doi.org/10.1128/AEM.01156-08.
45. Holt JG, Krieg NR, Sneath PHA. 1994. Bergey's manual of determinative bacteriology, 9th ed. Williams and Wilkins, Baltimore, MD.
46. Kimura M. 1980. A simple method for estimating evolutionary rates of base substitutions through comparative studies of nucleotide sequences. J Mol Evol 16:111–120. https://doi.org/10.1007/BF01731581.
47. Saitou N, Nei M. 1987. The neighbor-joining method: a new method for reconstructing phylogenetic trees. Mol Biol Evol 4:406–425.
48. Thompson JD, Higgins DG, Gibson TJ. 1994. CLUSTAL W: improving the sensitivity of progressive multiple sequence alignment through sequence weighting, position-specific gap penalties and weight matrix choice. Nucleic Acids Res 22:4673–4680.
49. White J. 1979. Spectrophotometric method for hydroxymethylfurfural in honey. J Assn Official Analyt Chemists 62:509–514.
50. Madani-Tonekabonia M, Kamankesha M, Mohammadi A. 2015. Determination of furfural and hydroxymethyl furfural from baby formula using dispersive liquid–liquid microextraction coupled with high performance liquid chromatography and method optimization by response surface methodology. J Food Compost Anal 40:1–7. https://doi.org/10.1016/j.jfca.2014.12.004.
51. Turner JH, Rebers PA, Barrick PL, Cotton RH. 1954. Determination of 5-(hydroxymethyl)-2-furaldehyde and related compounds. Anal Chem 26:898–901. https://doi.org/10.1021/ac60089a027.
52. Perutka J, Wang WJ, Goerlitz D, Lambowitz AM. 2004. Use of computer-designed group II introns to disrupt *Escherichia coli* DExH/D-box protein and DNA helicase genes. J Mol Biol 336:421–439. https://doi.org/10.1016/j.jmb.2003.12.009.
53. Jang YS, Lee JY, Lee J, Park JH, Im JA, Eom M-H, Lee J, Lee S-H, Song H, Cho J-H, Seung DY, Lee SY. 2012. Enhanced butanol production obtained by reinforcing the direct butanol-forming route in *Clostridium acetobutylicum*. mBio 3:e00314421–12. https://doi.org/10.1128/mBio.00314-12.
54. Li Y, Tschaplinski T, Engle N, Hamilton C, Rodriguez M, Liao J, Schadt C, Guss A, Yang Y, Graham D. 2012. Combined inactivation of the *Clostridium cellulolyticum* lactate and malate dehydrogenase genes substantially increases ethanol yield from cellulose and switch grass fermentations. Biotechnol Biofuels 5:2. https://doi.org/10.1186/1754-6834-5-2.
55. Thijs S, Van Hamme J, Gkorezis P, Rineau F, Weyens N, Vangronsveld J. 2014. Draft genome sequence of Raoultella ornithinolytica TNT, a trinitrotoluene-denitrating and plant growth-promoting strain isolated from explosive-contaminated soil. Genome Announc 2:e00491-14. https://doi.org/10.1128/genomeA.00491-14.
56. Abremski K, Wierzbicki A, Frommer B, Hoess RH. 1986. Bacteriophage P1 Cre-loxP site-specific recombination: site-specific DNA topoisomerase activity of the Cre recombination protein. J Biol Chem 261:391–396.
57. Hartung M, Kisters-Woike B. 1998. Cre mutants with altered DNA binding properties. J Biol Chem 273:22884–22891. https://doi.org/10.1074/jbc.273.36.22884.
58. Zhong J, Karberg M, Lambowitz AM. 2003. Targeted and random bacterial gene disruption using a group II intron (targetron) vector containing a retrotransposition-activated selectable marker. Nucleic Acids Res 31:1656–1664. https://doi.org/10.1093/nar/gkg248.
59. Lowry OH, Rosebrough NJ, Farr AL, Randall RJ. 1951. Protein measurement with the folin phenol reagent. J Biol Chem 193:265–275.
60. Bensadoun A, Weinstein D. 1976. Assay of proteins in the presence of interfering materials. Anal Biochem 70:241–250. https://doi.org/10.1016/S0003-2697(76)80064-4.
61. Kovach ME, Elzer PH, Hill DS, Robertson GT, Farris MA, Roop RM, II, Peterson KM. 1995. Four new derivatives of the broad-host-range cloning vector pBBR1MCS, carrying different antibiotic-resistance cassettes. Gene 166:175–176.